Development & Validation of Hindcast-Driven Nearshore Wave Information

William R. Dally and Daniel A. Osiecki

Surfbreak Engineering Sciences, Inc.
315 North Lakemont Avenue, Suite A
Winter Park, Florida 32792 U.S.A.
wdally@surfbreakengineering.com

1. Introduction

The Florida Department of Environmental Protection is sponsoring an investigative effort called the 'Florida Coastal Forcing Project' (FCFP), the purpose of which is to provide technical and scientific support for ongoing beach management and nourishment activities conducted by its Bureau of Beaches and Coastal Systems. One of the specific goals of the FCFP is the development of reliable methods for transforming available long-term deepwater hindcast information to the nearshore (~10m depth) for use in coastal engineering applications. To this end, a number of data collection and modeling activities have been conducted in the region south of Cape Canaveral, located on Florida's central Atlantic coast and shown in Figure 1. These activities include two data collection efforts: 1) ongoing measurement of directional wave spectra in the nearshore (~8.5m depth) at FCFP Station 'Spessard' (see Dally and Osiecki, 2005), and 2) limited-duration deployments of three additional wave gauges across the continental shelf seaward of Spessard (October, 2002 to March, 2003). The locations of the instruments from this 'Canaveral Cross-Shelf Experiment' (Liberty Tripod, Tug Tower, Rock Tower, and Spessard Station) are also shown in Figure 1.

The immediate objective of the study described herein is to replicate the ADCP-measured directional spectra obtained at the Spessard station, by transforming available deepwater hindcast information to the nearshore using 'STWAVE$^+$', which is a bottom-friction-enhanced version of the spectral wave transformation model STWAVE (Smith, Sherlock, and Resio, 2001). For deepwater-hindcast input, the 'AES' product (Swail and Cox, 2000) was selected due to 1) overlap of the AES archive with the measurements available from Spessard from August 28, 2001 to June 30, 2004, and 2) the potential to ultimately develop multi-decadal nearshore wave records from the 50-year-long AES database (July 1, 1954 to June 30, 2004). Although hindcast information is available from the latest generation of the Wave Information Study (WIS) developed by the U.S. Army Corps of Engineers, this database extends only from 1980 through 1999, and therefore does not overlap the available ADCP measurements. However, for reference, the locations of the latest WIS stations are also shown in Figure 1.

2. Bottom Friction Calibration of STWAVE$^+$ for the Canaveral Bight

Selection of the bottom friction coefficient required by STWAVE$^+$ was guided by data collected during the Canaveral Cross-Shelf Experiment. The objective was to use the directional spectra from the outermost gauge (Liberty Tripod) to drive STWAVE$^+$, and to use the concomitantly collected data from the innermost gauge (Spessard) to guide the calibration of the friction coefficient to a single, optimum value. Before proceeding however, the data had to be conditioned in several ways.

Firstly, the Liberty data were screened so as to use only those times when bottom friction was expected to be relatively strong. The purpose of this was to preclude, as much as possible, the use of bottom friction as a means of artificially compensating for any shortcomings that may exist in STWAVE's representation of other physical processes (e.g. whitecapping). Adopting a bed stress definition given by

$$\vec{\tau} = \rho \, C_f \; \vec{u} \left| \vec{u} \right| \tag{1}$$

a characterization of energy dissipation due to bottom friction was first computed using spectral parameters measured at the Liberty Tripod and the expression

$$\varepsilon_F = \frac{\frac{\sqrt{2}}{3} \, \pi^2 \, f_p^{\;3} \, H_{mo}^{\;\;3}}{\sinh^3 k_p h} \tag{2}$$

in which f_p is the peak wave frequency, H_{mo} is the energy-based significant wave height, k_p is the wave number associated with the peak frequency (T_p) and computed from linear wave theory, and h is a representative water depth, taken to be 14 m in the region of interest. Equation 2 provides an estimate that is proportional to the rate of energy dissipation per unit planform area.

Figure 2 provides a synopsis of the Liberty Tripod data from the first deployment (October 27 – November 25, 2002). The upper panel presents an intensity plot of the directional distribution of wave energy, as well as the wind direction from NDBC 41009. The second panel is wind speed. The third panel is the dissipation indicator computed from Eq. 2, using the peak period and significant wave height shown in the fourth and fifth panels respectively. The times when dissipation would be expected to be strongest are clearly evident, and a value of 0.01 m^2/s was adopted as a screening threshold.

STWAVE does not treat the physics of waves under opposing wind conditions, which in nature is manifest by an apparent loss in energy in the propagation direction (i.e. much like bottom friction). Consequently, the second screening criterion applied was to discard the times during which the wind was outside a directional window of $\pm 87.5^o$ from the peak of the directional distribution of energy.

In applying the two screening criteria described above, of the more than 1200 spectra measured at the Liberty Tripod, only 55 survived for use in calibrating STWAVE$^+$. In final preparation for conducting the calibration runs, because STWAVE$^+$ is a 'half-plane' model and treats waves from directions only within $\pm 87.5^o$ of grid-normal (73^o), the screened Liberty spectra were directionally trimmed to conform to this constraint.

For each of the 55 screened and trimmed input spectra, three runs of STWAVE$^+$ were performed, each with a different bed friction coefficient, 0.0 (i.e. no friction), 0.05, and 0.1, and the results archived at the location of the Spessard gauge. This range in friction factor was believed to encompass that which is typical for the offshore region of the Canaveral Bight. A histogram of the results for each of the three values of C_f is provided in Figure 3, as well as the histogram of targeted results from the measured Spessard spectra (upper panel). In developing the measured values of H_{mo}, the same half-plane directional window was applied for consistency with the STWAVE^{+} results. This figure indicates that the friction factor should be somewhere between 0.0 and 0.05.

To conclude the calibration process, a 'best fit' friction factor was calculated for each of the 55 screened input spectra by 1) fitting a parabola to the three H_{mo} values predicted at Spessard from the three model runs ($C_f = 0$, 0.05, and 0.1), and then 2) interpolating the parabola using the value of H_{mo} measured at Spessard during that sample time. If the best-fit value fell outside the range of 0.0-0.10, the case was discarded. Eight such cases were found, resulting in 47 estimates of the best-fit friction factor. A histogram of these results is presented in Figure 4, along with a histogram of the associated measured wave heights. The median value of the best-fit C_f (0.026) was subsequently adopted throughout the remainder of the study.

Using $C_f = 0.026$ everywhere in the model domain, sample STWAVE^{+} results for the first deployment are presented in Figure 5. Note that 1) the effect of bottom friction in reducing energy in the nearshore is evident only intermittently, as was foreshadowed in Figure 2, 2) peak wave period does not undergo significant change between Liberty and Spessard, and 3) wave direction is faithfully modeled at Spessard, indicating the effect of refraction in rotating the waves towards shore-normal, thereby compressing the directional window. These results are encouraging.

3. Reconstitution of AES Directional Spectra

Before the deepwater AES information could be used as the offshore boundary condition to drive the locally calibrated STWAVE^{+}, a methodology had to be devised for reconstituting the fully directional spectra based upon the spectral parameters available in the AES archive. Because AES does provide information on sea and swell components, a somewhat sophisticated scheme capable of constructing spectra with two directional peaks was developed. This scheme utilized seven of the available parameters: 1) sea energy, 2) swell energy, 3) sea peak period, 4) swell peak period, 5) vector mean direction for the sea, 6) vector mean direction for the swell, and 7) angular spreading coefficient for the entire spectrum. For each of the two components, the frequency distribution was modeled after the JONSWAP spectrum, with the shape factor set at γ=3.3. The directional spreading function was modeled after the Mitsuyazu distribution (see e.g. Ochi, 1998, p.42 & p.216). With this method, fully directional input spectra were generated from the AES parameters for the time period from August 28, 2001 to June 30, 2004, which were available every six hours.

4. Comparison of AES/STWAVE^{+} Results to Spessard Data

The AES grid node that was closest to the region of interest in the southern Canaveral Bight was #3198 (see Figure 1). However, because it was nearly 40 km offshore, a sequential grid system was required to keep the run-time of the STWAVE^{+} model manageable, while attaining the spatial detail needed in the nearshore. The outer corner of the outer grid was located at AES station 3198, and its inner boundary passed among the WIS stations 441-444. The grid size used in the outer domain was 400 m, whereas the inner grid was 150 m. A bed friction factor of 0.026 was assigned to every cell in the model.

Figure 6 presents a comparison of ADCP-measured and AES/ STWAVE$^+$-modeled results, in the form of the average of 3653 concurrent directional spectra available during the overlapping time period from 8/28/01 through 6/30/04. The AES/ STWAVE$^+$ results appear to overestimate the total average wave energy that strikes the coast (i.e. the volume under the spectral surface) when compared to the ADCP.

To investigate further, the Spessard data were directionally partitioned into northeast ($\theta \leq 69^o$), shore normal ($69^o \leq \theta \leq 77^o$), and southeast ($\theta \geq 77^o$) windows, using the peak direction from the directional distribution of wave energy. Figure 7 and Figure 8 present comparisons of the directional distributions and frequency spectra, respectively, from the model and the measurements. Figure 7 indicates that the surplus energy found in Figure 6 is distributed somewhat symmetrically around the peak direction in each window, except perhaps for slight bias from the southern quadrant of the shore-normal window. Figure 8 indicates that the surplus energy is typically apportioned to a range in frequency slightly above the peak frequency, but not in the high-frequency tail of the spectrum.

To investigate the source of the discrepancy between the AES/STWAVE$^+$ results and the nearshore measurements, a scatter plot of modeled versus measured H_{mo} is shown in Figure 9. This figure indicates a positive bias in the model when observed wave heights are small, perhaps less than 1.0 m. To ascertain whether it is caused by the STWAVE$^+$ wave transformation model or that it originates with the AES input condition, a comparison of the AES information to the measurements from NDBC # 41009 (located in Figure 1) is presented in Figure 10. Although NDBC #41009 and AES 3198 are not collocated, the similarity between this plot and that of Figure 9 indicates that the disparity, at least to a significant degree, is likely due to over-prediction by AES of the wave energy in deep water during low-energy conditions, and not due to a problem with STWAVE$^+$.

Screening the data used to generate Figures 6-8 for times when the ADCP-observed significant wave height was 1.0 m or greater allows further assessment. Results are presented in Figures 11-13, and model comparisons to the data show notable improvement. However, additional refinement in the spectral reconstitution methods, particularly in regard to the frequency distribution, is needed. Such refinement, coupled with correction of the AES energy bias, should lead to improved representation of the nearshore directional wave spectra.

A sample comparison of the time series of wave parameters from the model and the Spessard measurements is shown in Figure 14. With the exception of mean wave period, the parameters appear to track well. The offset in mean wave period is due to the shortcomings in the frequency-reconstitution method, which apparently does not apportion sufficient energy to the high frequency tail (see Figures 8 & 13).

5. Summary and Conclusions

A rational, objective method has been developed and tested for calibrating the spectral wave transformation model STWAVE$^+$ for energy losses induced by bottom friction. The method relies on paired wave gauge measurements from high-resolution ADCPs, with one instrument in deep water and the other in shallow water. Demonstration of the method indicates that a friction coefficient of 0.026 is suitable for wave transformation modeling in the Canaveral Bight.

Using the locally calibrated version of STWAVE$^+$, and fully directional spectra reconstituted from the parameters available in the AES archive as driving input, prediction of 34 months of spectral wave measurements in the nearshore at Spessard has been attempted. Comparison of the Spessard measurements to the results of AES/STWAVE$^+$ modeling for the time period from August 28, 2001 to June 30, 2004 confirms the basic veracity of this methodology, but indicates that two enhancements are warranted: 1) improvement of AES during low-energy conditions, and 2) improvement of the representation of the frequency distribution function used in reconstituting the 2D spectra from AES parameters. Such improvements must be guided by wave measurements made in deep water.

6. References

Dally, W.R., and Osiecki, D.A., 2005, 'Nearshore Wave and Current Measurements During Hurricane Jeanne,' Shore and Beach, V73, No.2-3, 29-33.

Ochi, M.K., 1998, Ocean Waves: The Stochastic Approach, Cambridge Ocean Technology Series 6, N.Y.

Smith, J.M., Sherlock, A.R., and Resio, D.T., 2001, " STWAVE: Steady-State Spectral Wave Model User's Manual for STWAVE, Version 3.0," U.S. Army Corps of Engineers, Coastal and Hydraulics Laboratory, ERDC/CHL SR-01-1.

Swail, V.R. and A.T. Cox, 2000, "On the use of NCEP/NCAR reanalysis surface marine wind fields for a long term north atlantic wave hindcast," J. Atmo. Tech., Vol 17, No.4, pp.532-545.

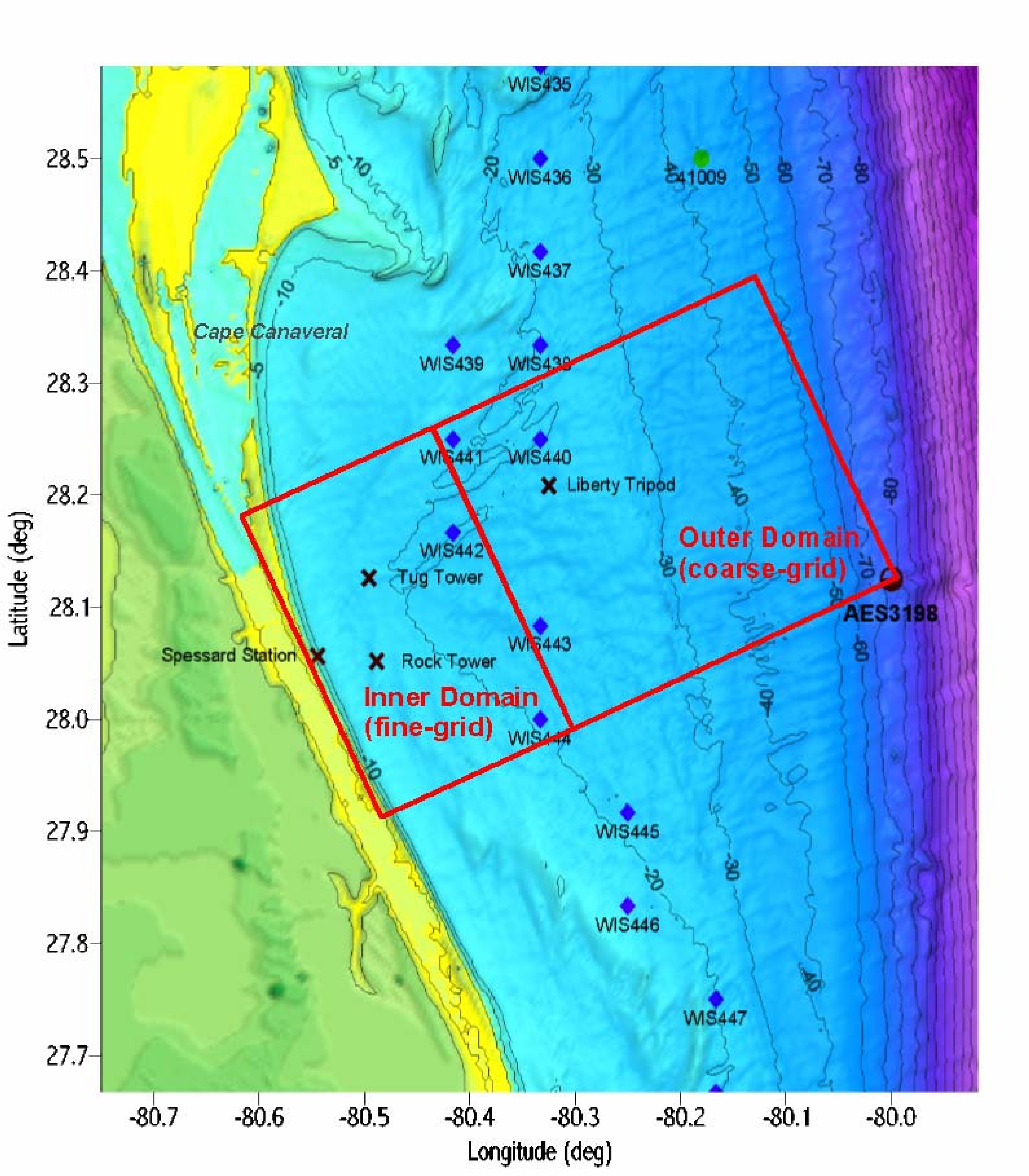

Figure 1 – Chart of Canaveral Bight showing locations of 1) FCFP Station Spessard, Rock Tower, Tug Tower, and Liberty Tripod, 2) AES grid point 3198, 3) NDBC buoy #41009 and 4) nested grid domains used in AES/STWAVE+ modeling of Spessard directional spectra. WIS Phase 3 stations are shown for reference. Depths in meters.

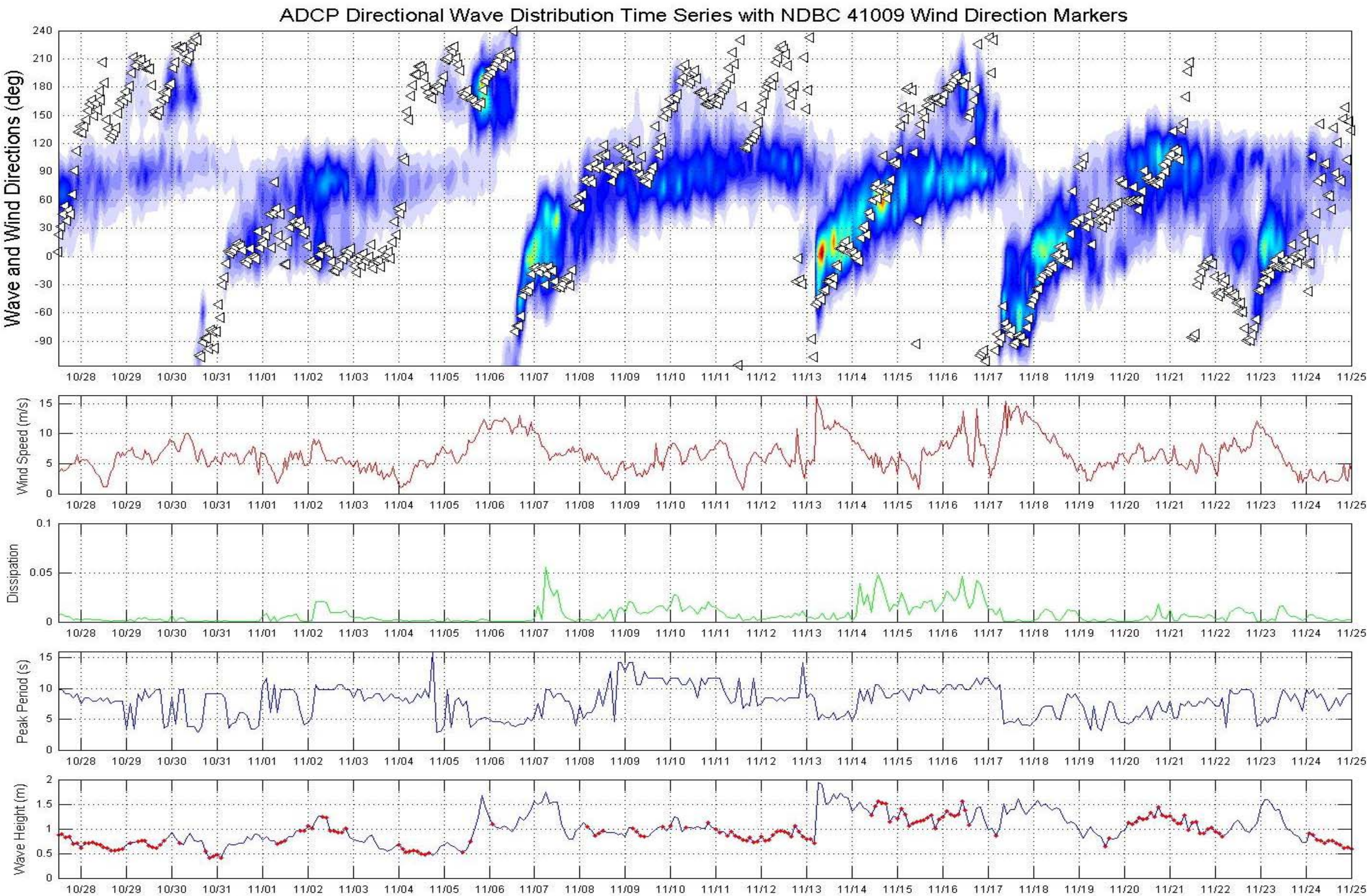

Figure 2 – Deepwater wave and wind information collected at the Liberty Tripod during the first deployment of the Canaveral Cross-Shelf Experiment. In the third panel, Eq. 2 is plotted as an indicator of dissipation due to bottom friction.

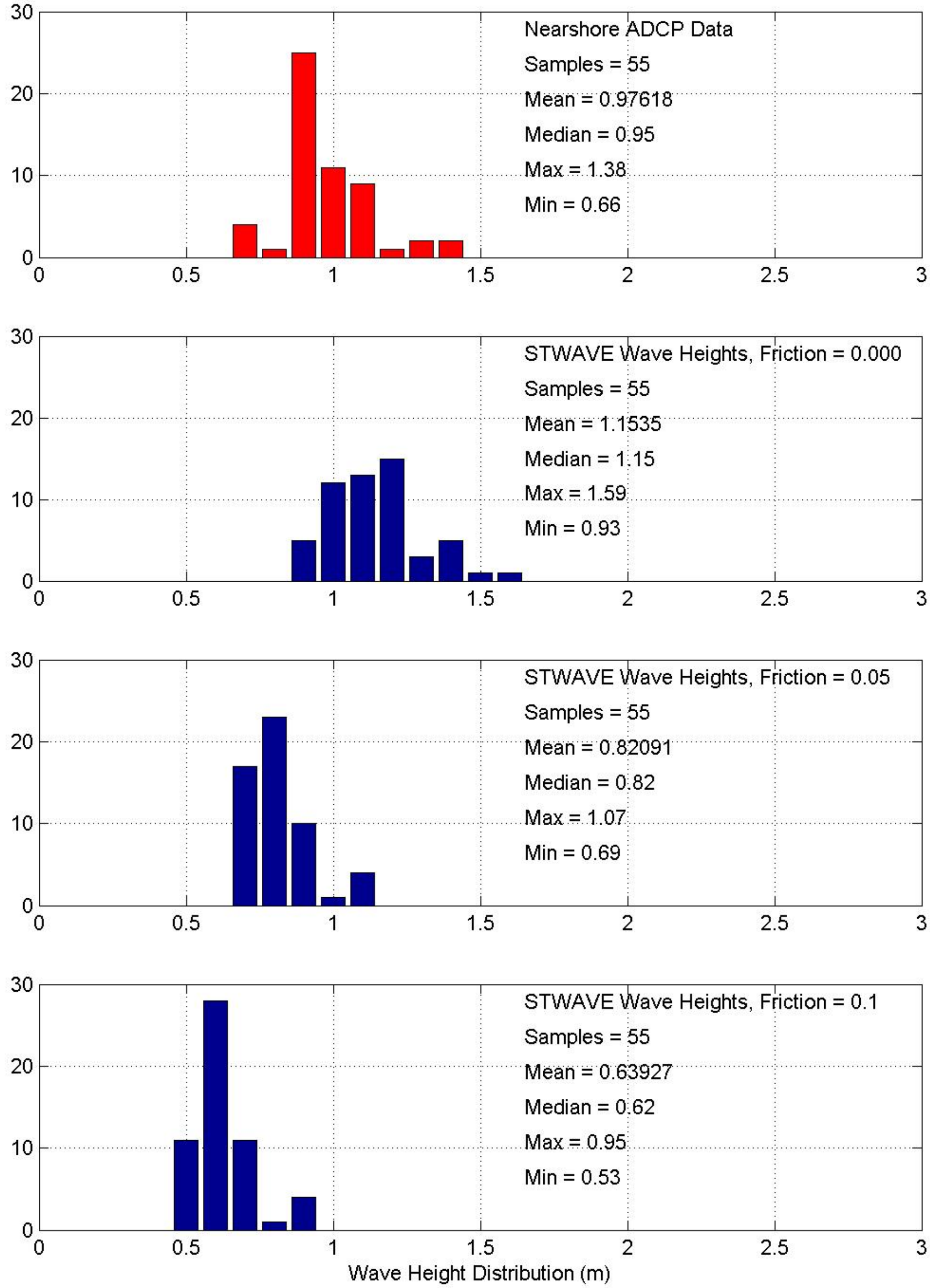

Figure 3 – Histogram of significant wave height from Spessard ADCP during the 55 samples when the screening criteria were satisfied (top) versus results from STWAVE$^+$ runs with differing bed friction coefficients.

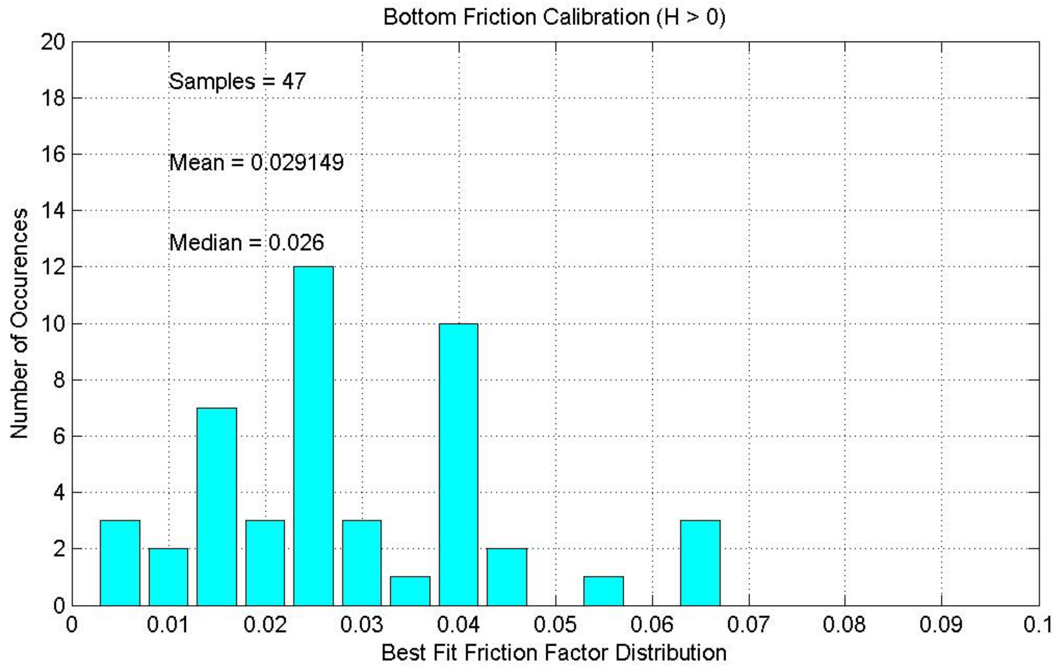

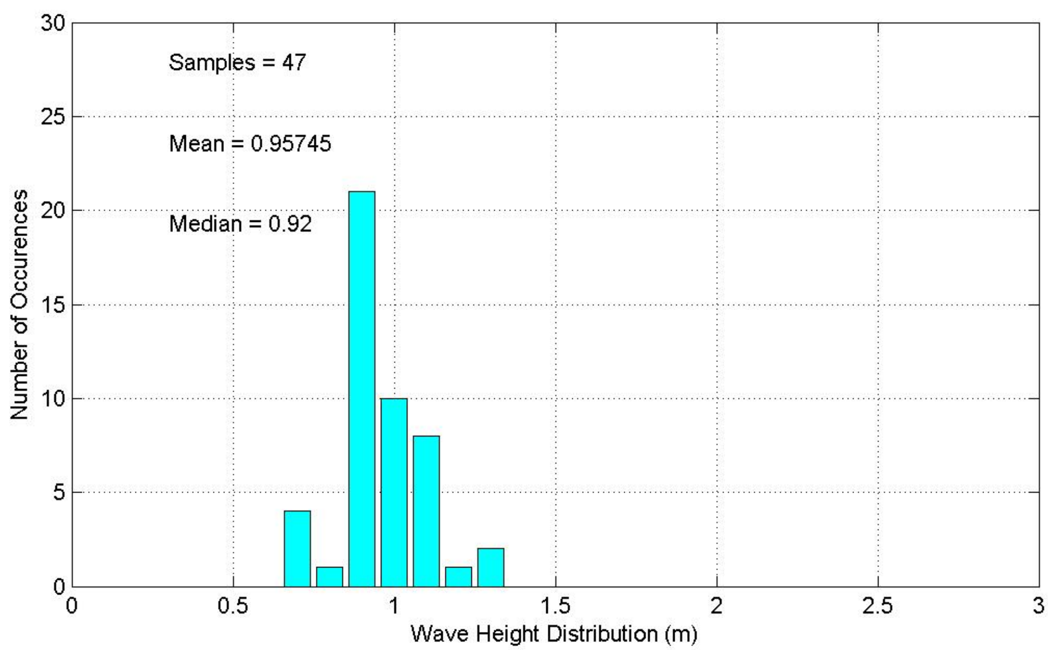

Figure 4 – Histogram of the 'best-fit' friction factor (top) and associated wave heights (bottom) determined from the STWAVE+ calibration exercise. Eight of the original 55 trials fell outside the range $0.0 < C_f < 0.1$ and were discarded.

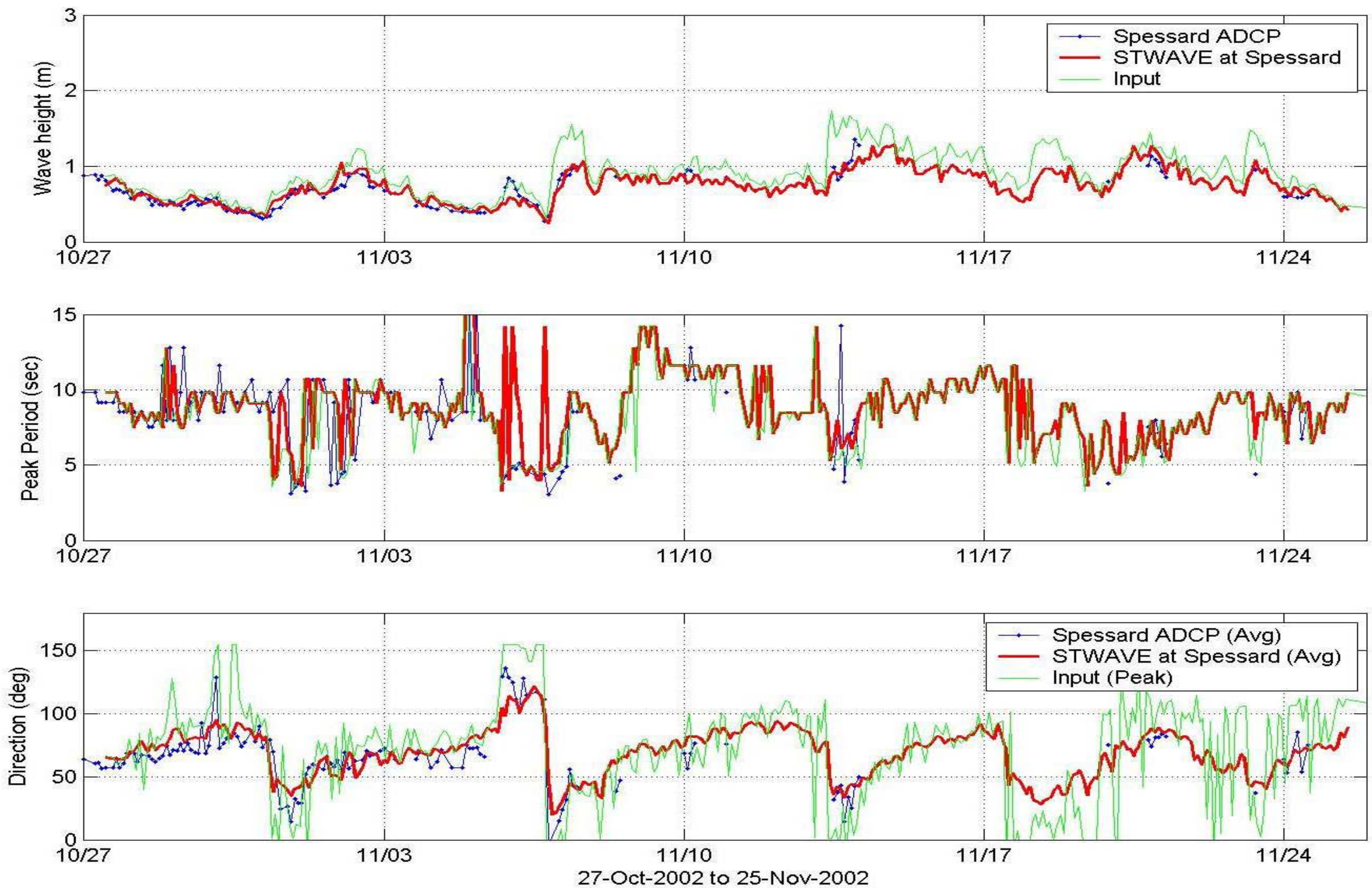

Figure 5 – Time series from first deployment of the Canaveral Cross-Shelf Experiment showing calibrated STWAVE+ results in comparison to ADCP measurements at Spessard. Input conditions from Liberty Tripod shown for reference.

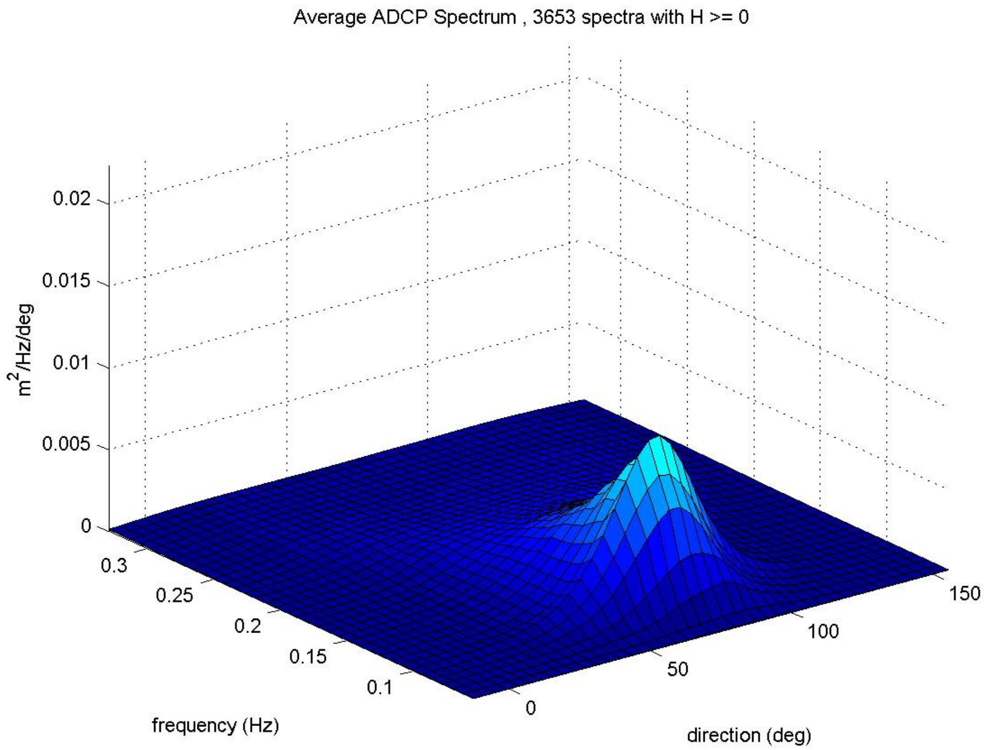

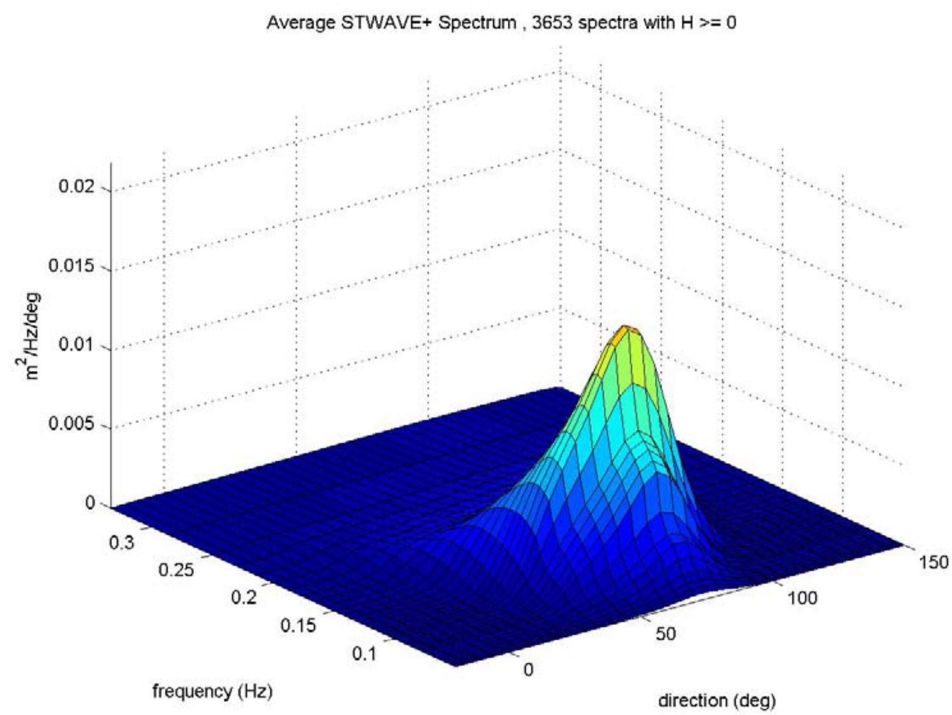

Figure 6 – Comparison of average 2D spectrum from AES/ STWAVE$^+$ to concurrent ADCP measurements for entire data set at Spessard.

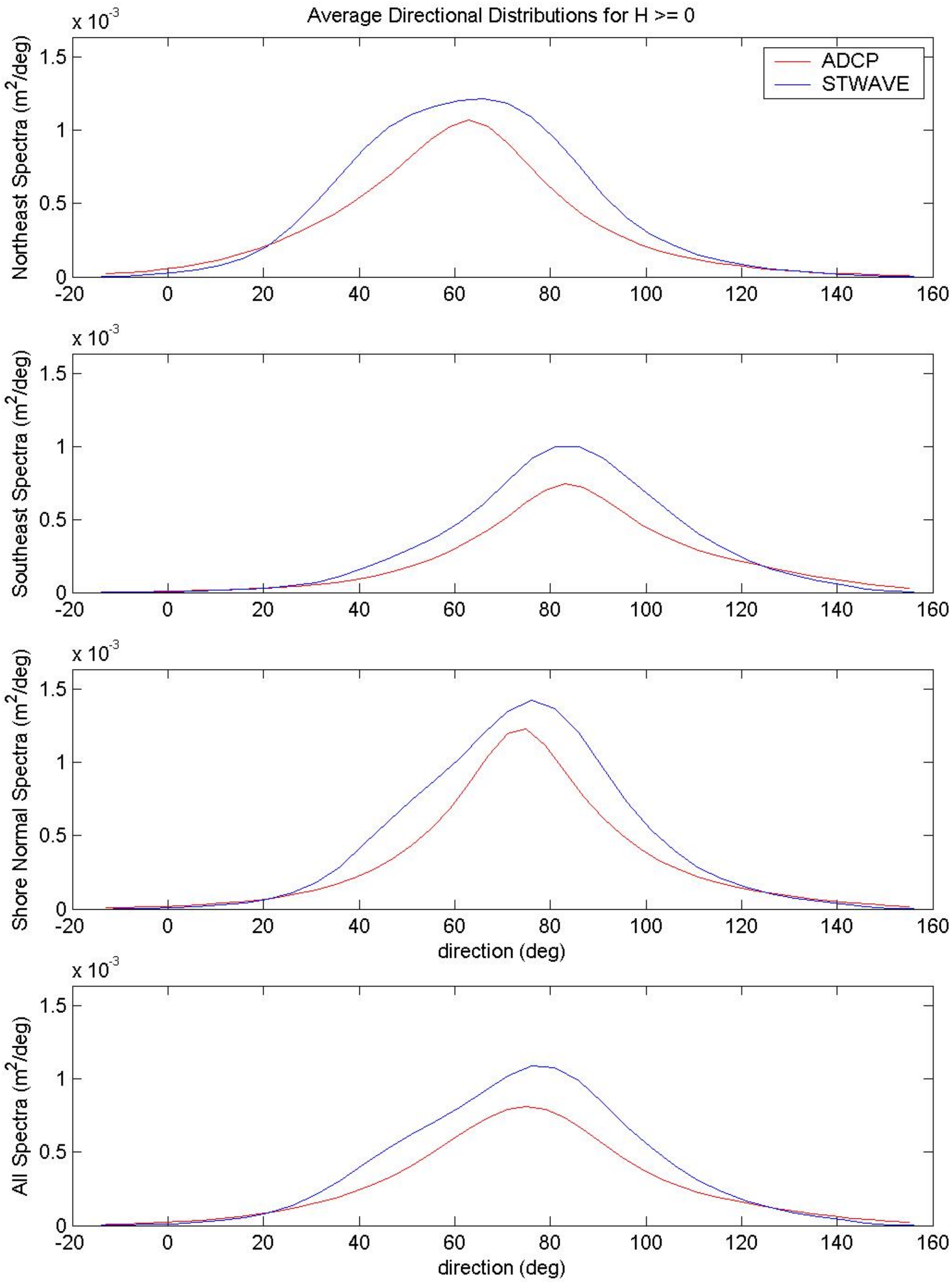

Figure 7 - Comparison of average directional distribution from AES/ STWAVE+ to concurrent ADCP measurements from Spessard.

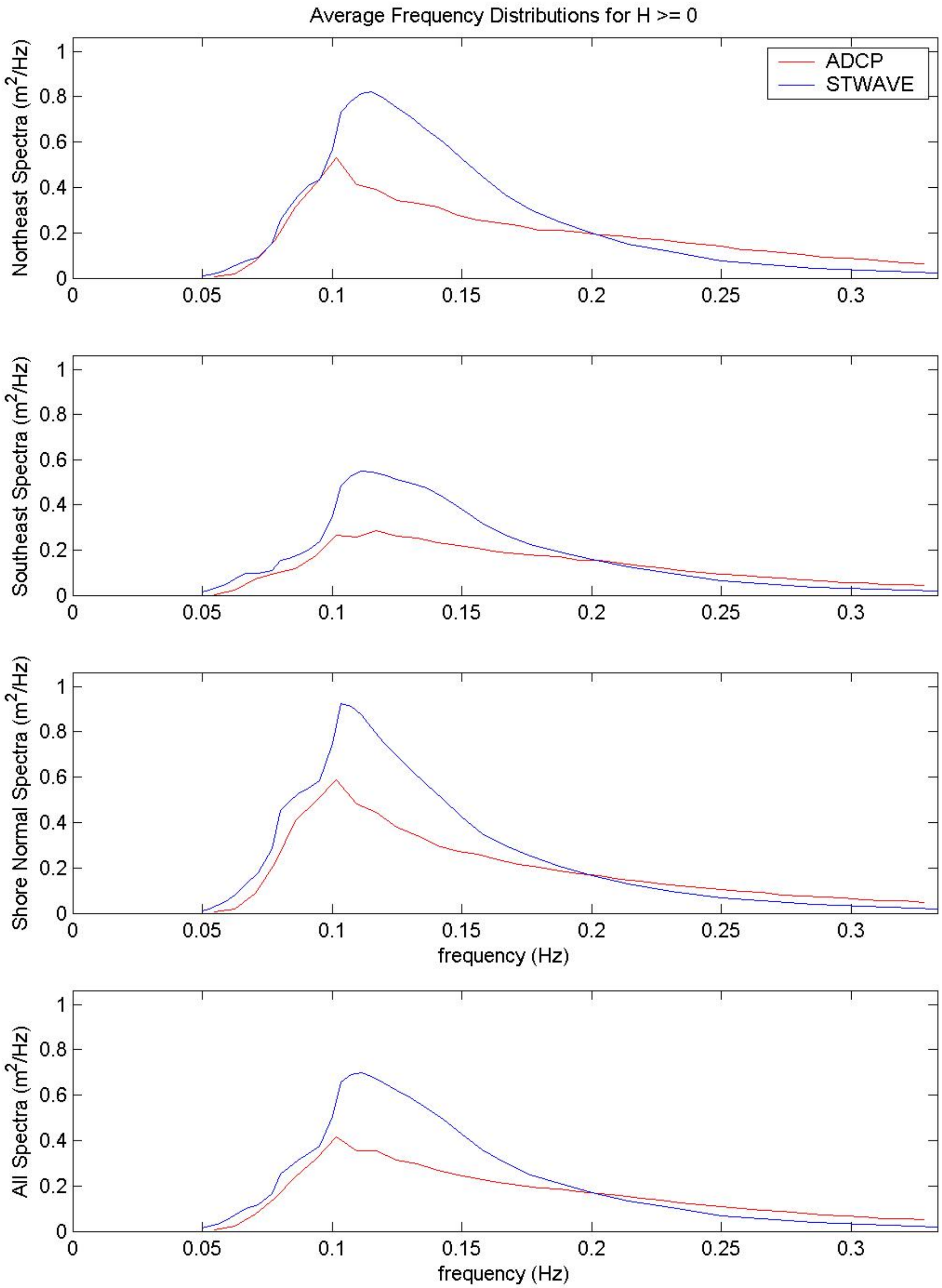

Figure 8 – Comparison of average frequency spectrum from AES/ STWAVE^{+} to concurrent ADCP measurements from Spessard.

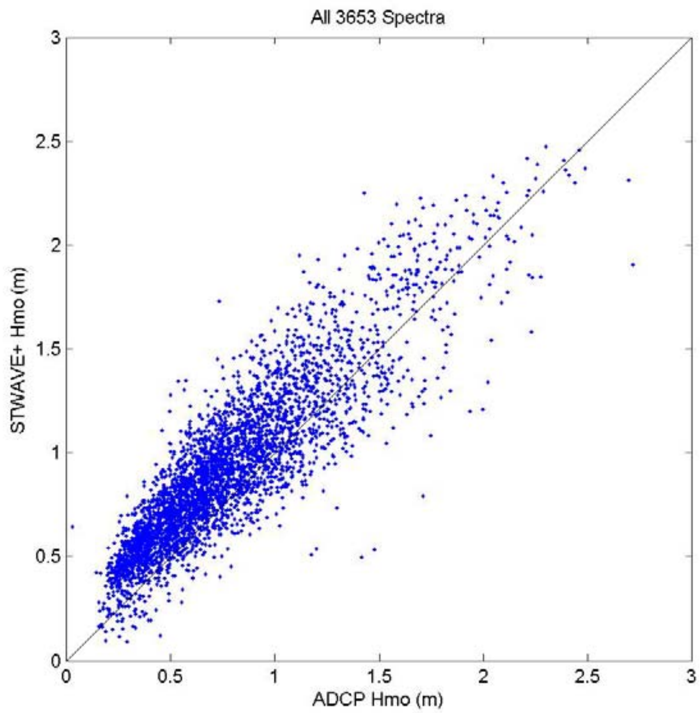

Figure 9 - Scatter plot of significant wave height from AES/STWAVE^{+} versus concurrent ADCP measurements at Spessard (August 28, 2001 - June 30, 2004).

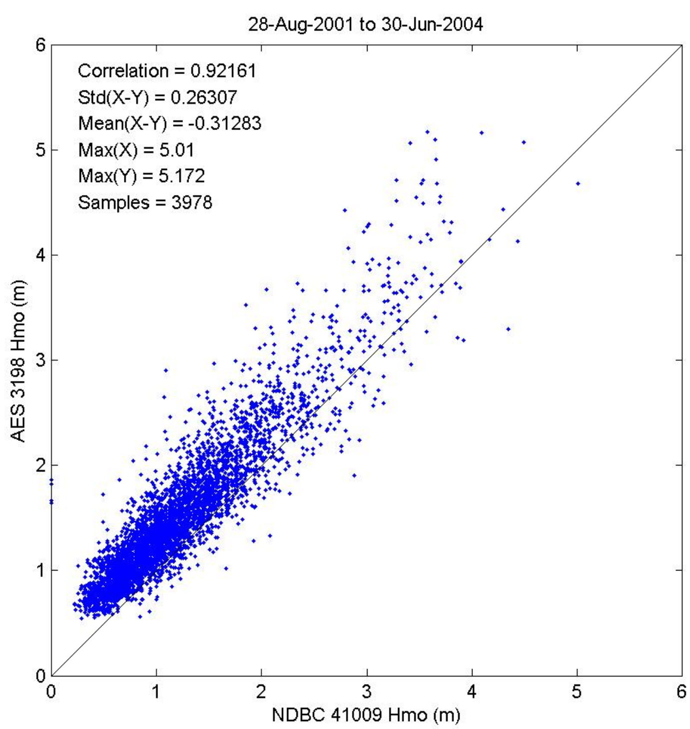

Figure 10 – Scatter plot of NDBC Buoy #41009 wave height measurements versus AES #3198 (August 28, 2001 to June 30, 2004).

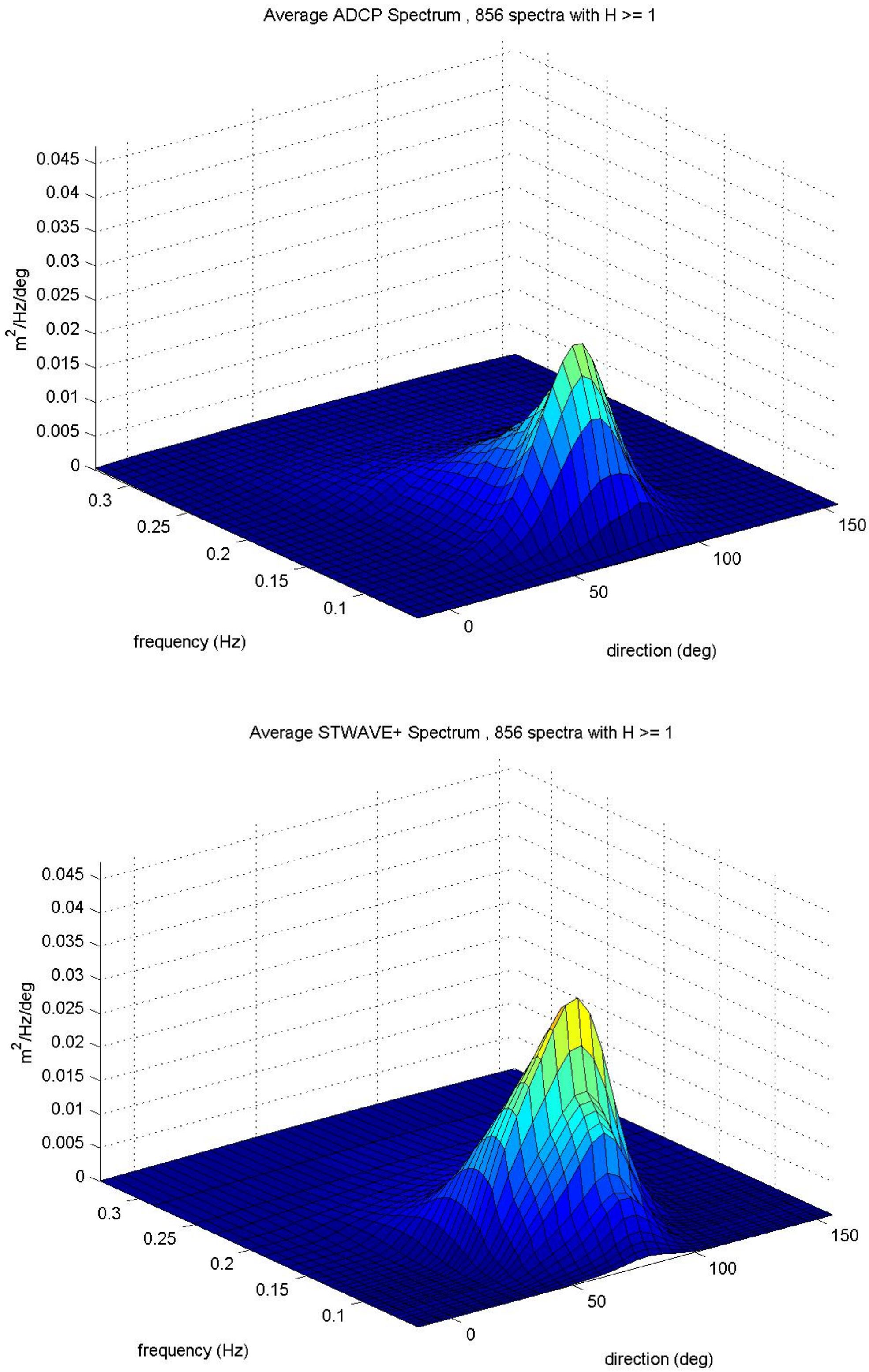

Figure 11 - Comparison of average directional spectra from AES/STWAVE$^+$ to ADCP measurements from Spessard, for significant wave heights greater than 1.0 m.

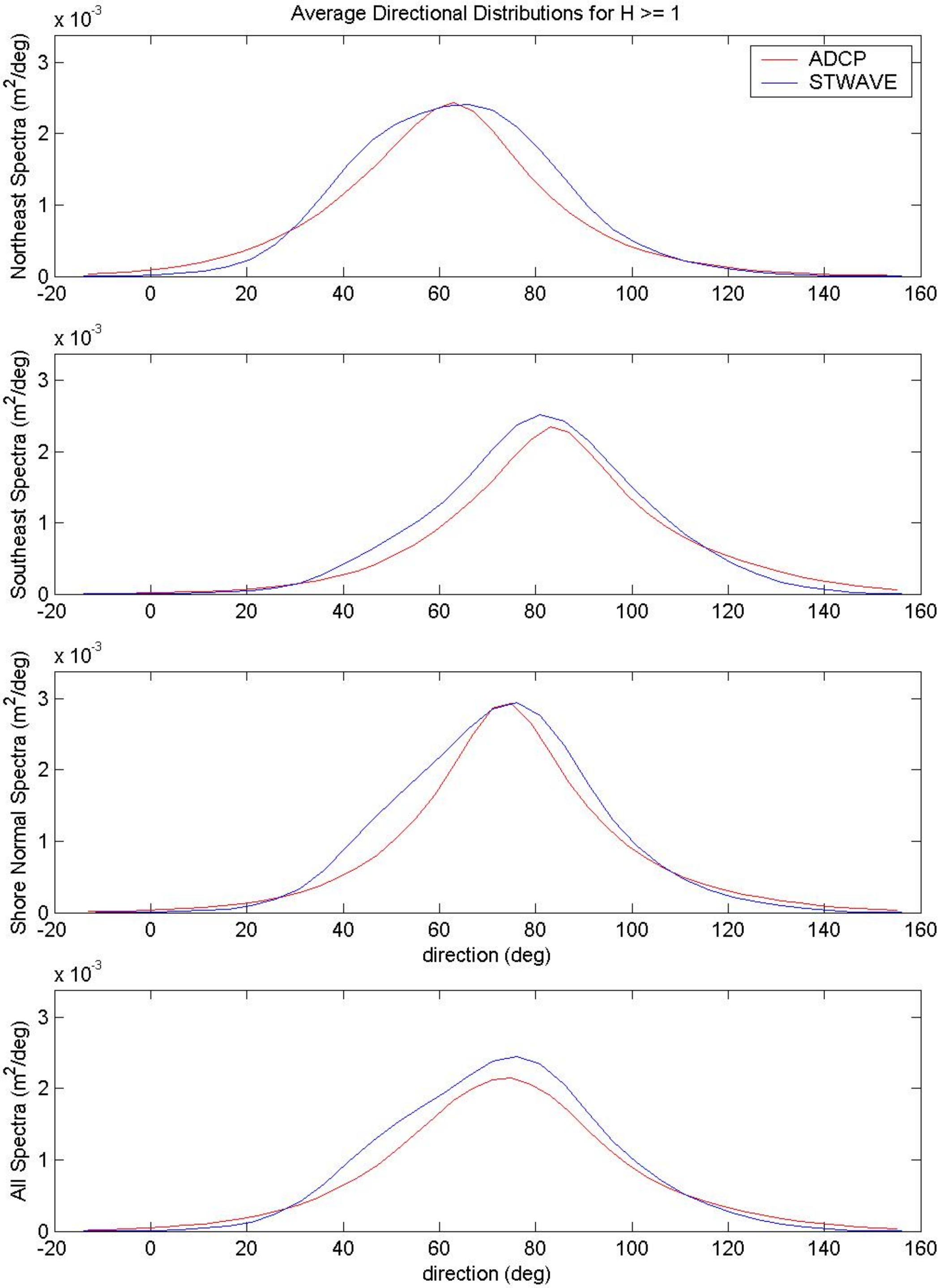

Figure 12 - Comparison of average directional distributions from AES/STWAVE+ to ADCP measurements from Spessard, for significant wave heights greater than 1.0 m.

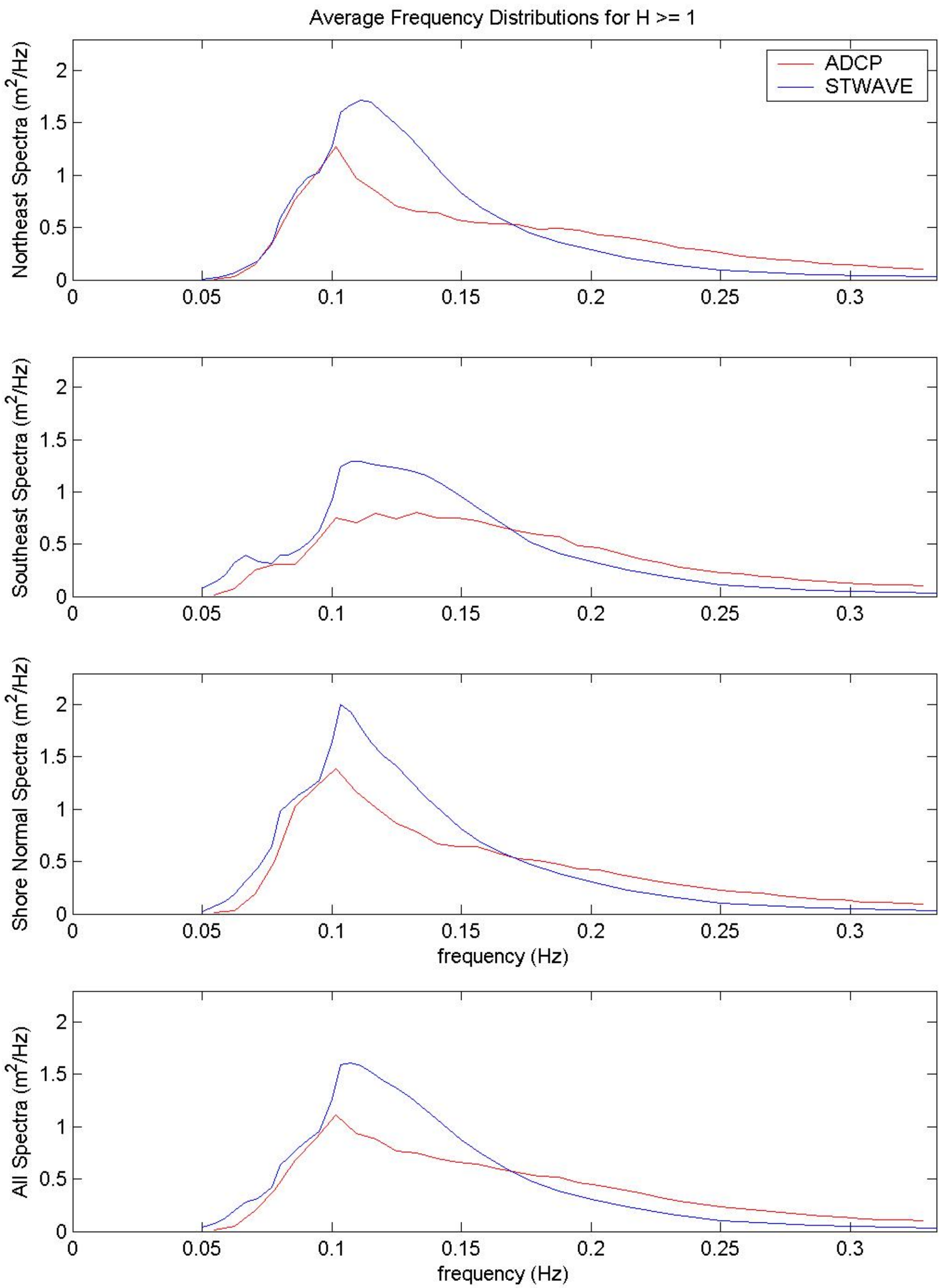

Figure 13 – Comparison of average frequency spectra from AES/STWAVE^{+} to ADCP measurements from Spessard, for significant wave heights greater than 1.0 m.

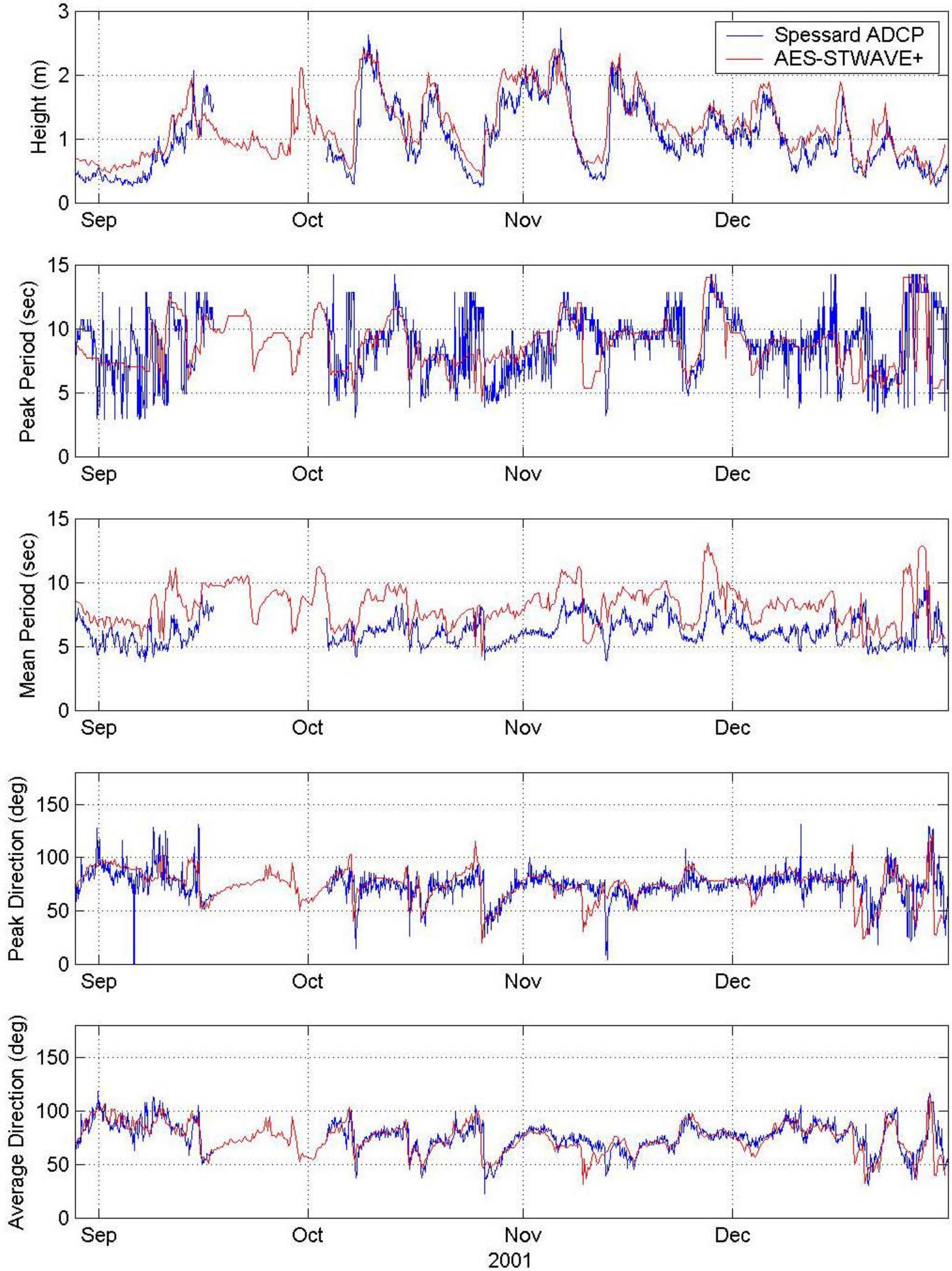

Figure 14 – Sample results of time-series of wave parameters from AES/STWAVE^{+} modeling to nearshore ADCP measurements from Spessard.